

Observation of New Charmonium or Charmoniumlike States in $B^+ \rightarrow D^{*\pm} D^\mp K^+$ Decays

R. Aaij *et al.**
(LHCb Collaboration)

 (Received 6 June 2024; accepted 13 August 2024; published 27 September 2024)

A study of resonant structures in $B^+ \rightarrow D^{*+} D^- K^+$ and $B^+ \rightarrow D^{*-} D^+ K^+$ decays is performed, using proton-proton collision data at center-of-mass energies of $\sqrt{s} = 7, 8,$ and 13 TeV recorded by the LHCb experiment, corresponding to an integrated luminosity of 9 fb^{-1} . A simultaneous amplitude fit is performed to the two channels with contributions from resonances decaying to $D^{*-} D^+$ and $D^{*+} D^-$ states linked by C parity. This procedure allows the C parities of resonances in the $D^{*\pm} D^\mp$ mass spectra to be determined. Four charmonium or charmoniumlike states are observed decaying into $D^{*\pm} D^\mp$: $\eta_c(3945)$, $h_c(4000)$, $\chi_{c1}(4010)$, and $h_c(4300)$, with quantum numbers J^{PC} equal to 0^{-+} , 1^{+-} , 1^{++} , and 1^{+-} , respectively. At least three of these states have not been observed previously. In addition, the existence of the $T_{\bar{c}\bar{s}0}^*(2870)^0$ and $T_{\bar{c}\bar{s}1}^*(2900)^0$ resonances in the $D^- K^+$ mass spectrum, already observed in the $B^+ \rightarrow D^+ D^- K^+$ decay, is confirmed in a different production channel.

DOI: [10.1103/PhysRevLett.133.131902](https://doi.org/10.1103/PhysRevLett.133.131902)

The observation of two open-charmed resonant structures $T_{\bar{c}\bar{s}0}^*(2870)^0$, and $T_{\bar{c}\bar{s}1}^*(2900)^0$, consistent with tetraquark states with minimal quark content $[\bar{c}\bar{s}ud]$, was reported by the LHCb Collaboration in the $B^+ \rightarrow D^+ D^- K^+$ decay [1,2]. (The inclusion of charge conjugate processes is implied throughout the Letter, unless otherwise specified. The hadron naming scheme of Ref. [3] is used.) Confirmation of these states in other processes is critical to further establish their existence and improve understanding of their nature. Later, a pair of open-charmed exotic hadrons, one doubly charged and one neutral, was observed decaying to $D_s^+ \pi^\pm$ in the $B^+ \rightarrow D^- D_s^+ \pi^+$ and $B^0 \rightarrow \bar{D}^0 D_s^+ \pi^-$ processes, with quark contents $[c\bar{s}u\bar{d}]$ and $[\bar{c}\bar{s}\bar{u}d]$ [4,5], respectively. The $B^+ \rightarrow D^{*+} D^- K^+$ and $B^+ \rightarrow D^{*-} D^+ K^+$ decays are clean processes to search for open-charmed exotic states, as conventional excited D_s^+ mesons can not be formed in them. In addition, these decays are useful for investigation of charmonium or charmoniumlike states decaying into $D^{*\pm} D^\mp$. Among the observed charmonium(like) states, more than a dozen cannot be interpreted as $c\bar{c}$ charmonium states in the quark model [6–8]. However, few measurements have been made of charmonium(like) states decaying to $D^{*\pm} D^\mp$. In the studies that have been performed, the $X(3940)$ state was seen in $e^+ e^- \rightarrow J/\psi D^{*0/+} \bar{D}^{0/-}$ [9,10], and the

$T_{c\bar{c}1}(3900)^0$ state was seen in $e^+ e^- \rightarrow \pi^0 D^{*0/+} \bar{D}^{0/-}$ [11] processes, both of which exploit $e^+ e^-$ annihilations and therefore cannot be used to explore the full possible range of J^{PC} quantum numbers. Studies in B decays are of special interest as the different production mechanism to that of $e^+ e^-$ collisions may affect the rates of charmonium(like) states, providing opportunities to both understand the nature of already observed states and to uncover new ones.

In this Letter, the results of a simultaneous analysis of the $B^+ \rightarrow D^{*+} D^- K^+$ and $B^+ \rightarrow D^{*-} D^+ K^+$ decays are presented. The analysis is based on proton-proton (pp) collision data collected by the LHCb experiment, corresponding to an integrated luminosity of 9 fb^{-1} . Because of C -parity conservation in strong decays, any single charmonium(like) resonance R must contribute equally to the $B^+ \rightarrow R(D^{*+} D^-) K^+$ and $B^+ \rightarrow R(D^{*-} D^+) K^+$ processes, but interference between resonances with different C parity can result in differences between the two final states. By linking the decay amplitudes for $B^+ \rightarrow R(D^{*+} D^-) K^+$ and $B^+ \rightarrow R(D^{*-} D^+) K^+$ by C parity, one can determine the C parities of the resonances. This method is implemented for the first time in the analysis reported here.

The LHCb detector is a single-arm forward spectrometer covering the pseudorapidity range $2 < \eta < 5$, described in detail in Refs. [12,13]. It is designed specifically for the study of particles containing b or c quarks. Simulation is required to model the effects of the detector acceptance and the imposed selection requirements. In the simulation, pp collisions are generated using PYTHIA [14] with a specific LHCb configuration [15]. Decays of unstable particles are described by EvtGen [16], in which final-state radiation is generated using PHOTOS [17]. The interaction of the

*Full author list given at the end of the Letter.

Published by the American Physical Society under the terms of the [Creative Commons Attribution 4.0 International license](https://creativecommons.org/licenses/by/4.0/). Further distribution of this work must maintain attribution to the author(s) and the published article's title, journal citation, and DOI. Funded by SCOAP³.

generated particles with the detector and its response are implemented using the GEANT4 toolkit [18] as described in Ref. [19].

The same selection criteria as in a previous measurement of the branching fractions of $B^+ \rightarrow D^{*+}D^-K^+$ and $B^+ \rightarrow D^{*-}D^+K^+$ decays [20] are used. Charmed mesons are reconstructed using the $D^{*-} \rightarrow \bar{D}^0\pi^-$, $\bar{D}^0 \rightarrow K^+\pi^-$, $\bar{D}^0 \rightarrow K^+\pi^-\pi^-\pi^+$, and $D^- \rightarrow K^+\pi^-\pi^-$ decays. Preselections are applied to identify well-reconstructed tracks displaced from primary vertices of pp collisions and with large transverse momenta. Charmed meson candidates are required to have reconstructed masses consistent with the known values [6] and to have high-quality reconstructed vertices. Requirements are also applied on the quality of the B -candidate decay vertex and its displacement from any primary vertex. A multivariate classifier, based on a boosted decision tree [21,22] algorithm in the TMVA toolkit [23], is employed to further reduce combinatorial backgrounds using topological and particle identification information. In addition, backgrounds with one or zero charmed mesons in the final states are reduced by requiring the reconstructed $D^{0/+}$ candidates to have a significant flight distance from the B^+ decay vertex. The selected sample is divided into subsamples corresponding to two LHC run periods and different \bar{D}^0 and B^+ decay modes. For each subsample, a fit is performed to the $M(D^{*\pm}D^\mp K^+)$ distribution in the mass range [5210,5390] MeV to estimate the background fraction, f_{bg} , in the signal region defined as $M(D^{*\pm}D^\mp K^+) \in [5260, 5300]$ MeV, as done in the previous branching fraction measurement [20]. (Natural units with $\hbar = c = 1$

are used throughout the Letter.) In total, 1636 ± 43 and 1772 ± 44 signal decays are found in the signal region for the $B^+ \rightarrow D^{*+}D^-K^+$ and $B^+ \rightarrow D^{*-}D^+K^+$ decay modes, respectively, both with a background fraction of around 5%.

A subsequent amplitude fit, using an unbinned maximum-likelihood method, is performed simultaneously on the four subsamples. The log-likelihood (LL) for each subsample is defined as

$$\ln L = \sum_i \ln \left[(1 - f_{\text{bg}}) \frac{|\mathcal{A}(x_i)|^2}{\int |\mathcal{A}(x)|^2 \epsilon(x) d\Phi(x)} + f_{\text{bg}} \frac{B(x_i)}{\epsilon(x_i)} \right], \quad (1)$$

where x_i is a point in the phase space (Φ) for candidate i of the considered decay. The normalization factors are calculated using simulated samples [24], from which the efficiency $\epsilon(x)$ is obtained by applying the same criteria as used for data, and correcting for data-simulation differences in the particle identification [25], tracking [26], and trigger response [27]. The background fraction f_{bg} is fixed to the value from the preceding mass fit. The function $B(x)$ is the background probability density function. The background probability density function is modeled using candidates in the B -candidate mass sideband regions, $M(D^{*\pm}D^\mp K^+) \in [5220, 5240]$ or $[5320, 5340]$ MeV.

The amplitude $\mathcal{A}(x)$ is the coherent sum of all resonant and nonresonant (NR) contributions, denoted with subscripts j, k, l for resonances decaying into different final states,

$$\begin{aligned} \mathcal{A}(x) = & \frac{1+d}{2} \left\{ \sum_{j \in R(D^{*\pm}D^\mp)} c_j A_j(x) + \sum_{k \in R(D^{*-}K^+, D^+K^+)} c_k A_k(x) \right\} \\ & + \frac{1-d}{2} \left\{ \sum_{j \in R(D^{*\pm}D^\mp)} C_j \times c_j A_j(x) + \sum_{l \in R(D^{*+}K^+, D^-K^+)} c_l A_l(x) \right\}, \quad (2) \end{aligned}$$

where $d = +1$ for $B^+ \rightarrow D^{*-}D^+K^+$ decays and $d = -1$ for $B^+ \rightarrow D^{*+}D^-K^+$ decays. The C parity of the resonance R is denoted as C_j . The branching fractions of $B^+ \rightarrow RK^+$ decays followed by $R \rightarrow D^{*+}D^-$ and $R \rightarrow D^{*-}D^+$ states are equal, guaranteed by C -parity conservation in strong decays of the resonance R . No such constraints are applied on the amplitudes for resonances decaying into $D^{*\mp}K^+$ or $D^\pm K^+$ states. The complex coefficients $c_{j/k/l}$ are determined from the fit to data, with one of them fixed to unity as a reference. The amplitude of each resonance, $A_{j/k/l}(x)$, is constructed using the helicity formalism.

Both S -wave and D -wave amplitudes contribute significantly to the decays $R \rightarrow D^{*\pm}D^\mp$ when R has spin parity $J^P = 1^+$. The line shapes for these partial waves are described by

$$f_{R,S/D}(m) = \frac{\gamma_{S/D}}{m_0^2 - m^2 - im_0[\gamma_S^2 \Gamma_S(m) + \gamma_D^2 \Gamma_D(m)]}, \quad (3)$$

where γ_S and γ_D denote S - and D -wave coupling constants determined from the fit, with normalization condition $\gamma_S^2 + \gamma_D^2 = 1$. The mass-dependent width is

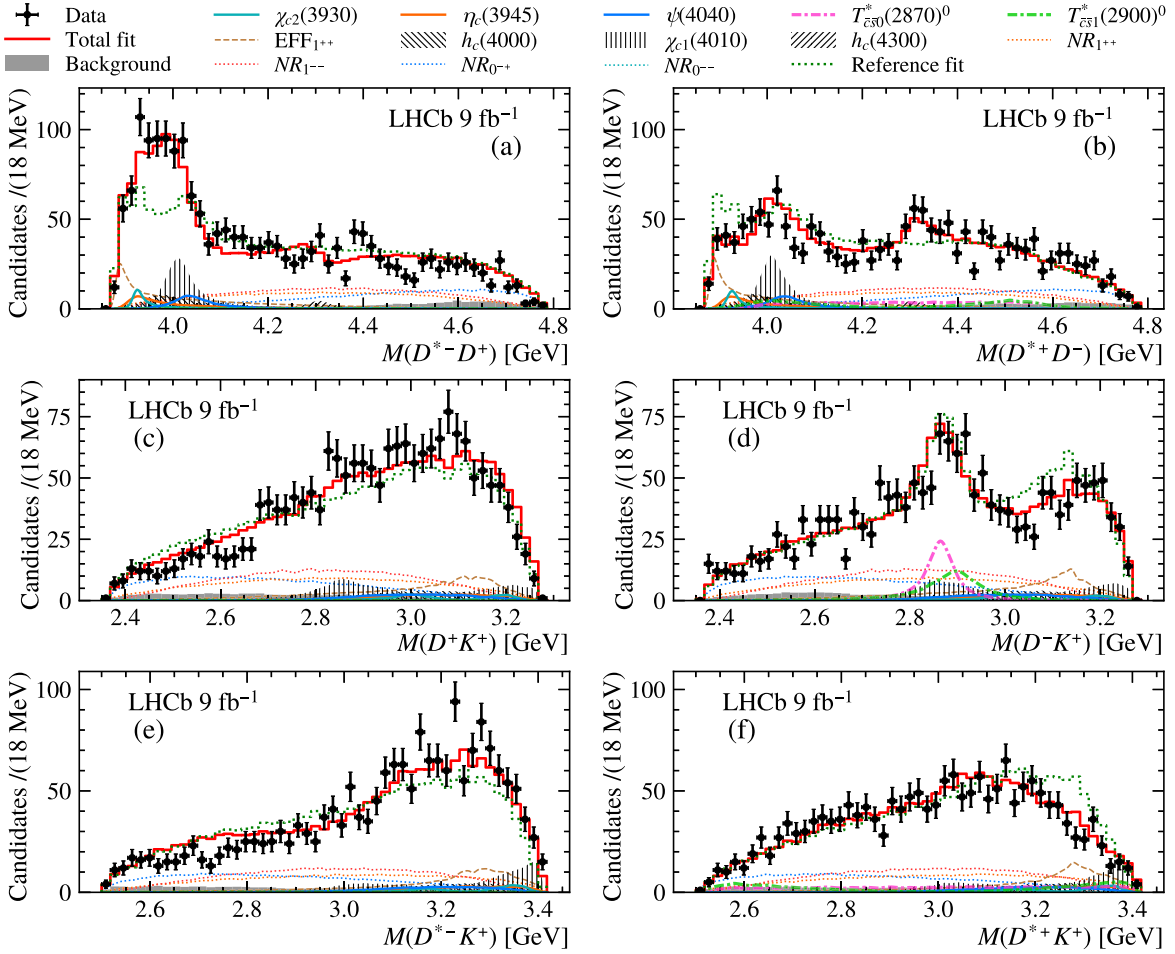


FIG. 1. Distributions of two-body invariant masses. (a) $M(D^{*-}D^+)$, (c) $M(D^+K^+)$, and (e) $M(D^{*-}K^+)$ in the $B^+ \rightarrow D^{*-}D^+K^+$ sample; (b) $M(D^+D^-)$, (d) $M(D^-K^+)$, and (f) $M(D^{*+}K^+)$ in the $B^+ \rightarrow D^{*+}D^-K^+$ sample. The fit results (red solid lines) are overlaid on the data distributions. Contributions from different components are also shown in different line styles as indicated in the legend. The result of fitting the data using a model without the $h_c(4000)$, $\chi_{c1}(4010)$, and $h_c(4300)$ components (reference fit) is shown with green dotted lines for comparison.

$\Gamma(m) = \Gamma_0(m_0/m)(q/q_0)^{2l+1}B_l^2(q, q_0, d)$, where l corresponds to the angular momentum between the two decay products of the resonance R , $B_l^2(q, q_0, d)$ is the Blatt-Weisskopf barrier factor [28] with $d = 3.0 \text{ GeV}^{-1}$, q (q_0) denotes the momentum of the decay products in the rest frame of the resonance at the reconstructed mass m (pole mass m_0), and Γ_0 is the width of the resonance. For all other resonances, the Breit-Wigner function $f_R(m) = 1/[m_0^2 - m^2 - im_0\Gamma(m)]$ is used. An *ad hoc* formula [29] is used to calculate q_0 if m_0 is smaller than the $M(D^{*\pm}D^\mp)$ threshold.

A large range of possible models are fitted to data, with the LL value used as the primary measure of relative goodness of fit, assisted by binned χ^2 tests. The final baseline model includes only components that are found to have significances above 5σ . The significance is determined either based on LL difference between fits including or not the component if the added resonance

was not observed before, or using ensembles of pseudo-experiments to take into account “look-elsewhere effects” if not [30,31].

The outcome of the fit with the baseline model is compared to data in Fig. 1, where clear differences are seen in the $M(D^{*+}D^-)$ and $M(D^{*-}D^+)$ spectra around 4.0 GeV due to different interference behaviors. Numerical results and a list of the resonances included in the model are given in Table I. The parameters of the $\chi_{c2}(3930)$, $\psi(4040)$, $T_{\bar{c}s0}^*(2870)^0$, and $T_{\bar{c}s1}^*(2900)^0$ resonances are fixed to their known values [6], while those of other states are allowed to vary freely in the fit.

At the $D^{*\pm}D^\mp$ threshold, a 1^{++} contribution is needed to describe the spectrum. Different effective models ($\text{EFF}_{1^{++}}$) are tried including exponential NR line shapes and tails of a $\chi_{c1}(3872)$ component modeled by Eq. (3) with mass and width parameters fixed to the known values [6]. These two line shapes give similar fit qualities. A model-independent

TABLE I. Resonant and nonresonant components included in the baseline fit and their spin parities, fit fractions, and product branching fractions [$\mathcal{B}(B^+ \rightarrow RC) \times \mathcal{B}(R \rightarrow AB)$], where A, B, C are the three final-state particles. To obtain the branching fractions, including both $R \rightarrow D^{*+}D^-$ and $R \rightarrow D^{*-}D^+$, the values in the table should be multiplied by a factor of 2. The first uncertainties are statistical, estimated with a bootstrap method [32], the second are systematic, and the third are from the uncertainty of the $B^+ \rightarrow D^{*+}D^-K^+$ branching fraction. The masses and widths of the resonances marked with the \dagger symbol are fixed to their known values [6].

Component	$J^{P(C)}$	Fit fraction [%] $B^+ \rightarrow D^{*+}D^-K^+$	Fit fraction [%] $B^+ \rightarrow D^{*-}D^+K^+$	Branching fraction [10^{-4}]
EFF $_{1^{++}}$	1^{++}	$10.9^{+2.3}_{-1.2} {}^{+1.6}_{-2.1}$	$9.9^{+2.1}_{-1.0} {}^{+1.4}_{-1.9}$	$0.74^{+0.16}_{-0.08} {}^{+0.11}_{-0.14} \pm 0.07$
$\eta_c(3945)$	0^{-+}	$3.4^{+0.5}_{-1.0} {}^{+1.9}_{-0.7}$	$3.1^{+0.5}_{-0.9} {}^{+1.7}_{-0.6}$	$0.23^{+0.04}_{-0.07} {}^{+0.13}_{-0.05} \pm 0.02$
$\chi_{c2}(3930)^\dagger$	2^{++}	$1.8^{+0.5}_{-0.4} {}^{+0.6}_{-1.2}$	$1.7^{+0.5}_{-0.4} {}^{+0.6}_{-1.1}$	$0.12^{+0.03}_{-0.03} {}^{+0.04}_{-0.08} \pm 0.01$
$h_c(4000)$	1^{+-}	$5.1^{+1.0}_{-0.8} {}^{+1.5}_{-0.8}$	$4.6^{+0.9}_{-0.7} {}^{+1.4}_{-0.7}$	$0.35^{+0.07}_{-0.05} {}^{+0.10}_{-0.05} \pm 0.03$
$\chi_{c1}(4010)$	1^{++}	$10.1^{+1.6}_{-0.9} {}^{+1.3}_{-1.6}$	$9.1^{+1.4}_{-0.8} {}^{+1.2}_{-1.4}$	$0.69^{+0.11}_{-0.06} {}^{+0.09}_{-0.11} \pm 0.06$
$\psi(4040)^\dagger$	1^{--}	$2.8^{+0.5}_{-0.4} {}^{+0.5}_{-0.5}$	$2.6^{+0.5}_{-0.4} {}^{+0.4}_{-0.5}$	$0.19^{+0.04}_{-0.03} {}^{+0.03}_{-0.03} \pm 0.02$
$h_c(4300)$	1^{+-}	$1.2^{+0.2}_{-0.5} {}^{+0.2}_{-0.2}$	$1.1^{+0.2}_{-0.5} {}^{+0.2}_{-0.2}$	$0.08^{+0.01}_{-0.03} {}^{+0.02}_{-0.01} \pm 0.01$
$T_{\bar{c}\bar{s}0}^*(2870)^{0,\dagger}$	0^+	$6.5^{+0.9}_{-1.2} {}^{+1.3}_{-1.6}$...	$0.45^{+0.06}_{-0.08} {}^{+0.09}_{-0.10} \pm 0.04$
$T_{\bar{c}\bar{s}1}^*(2900)^{0\dagger}$	1^-	$5.5^{+1.1}_{-1.5} {}^{+2.4}_{-1.6}$...	$0.38^{+0.07}_{-0.10} {}^{+0.16}_{-0.11} \pm 0.03$
NR $_{1^{--}}(D^{*\mp}D^\pm)$	1^{--}	$20.4^{+2.3}_{-0.6} {}^{+2.1}_{-2.6}$	$18.5^{+2.1}_{-0.5} {}^{+1.9}_{-2.3}$	$1.39^{+0.16}_{-0.04} {}^{+0.14}_{-0.17} \pm 0.12$
NR $_{0^{--}}(D^{*\mp}D^\pm)$	0^{--}	$1.2^{+0.6}_{-0.1} {}^{+0.7}_{-0.6}$	$1.1^{+0.6}_{-0.1} {}^{+0.6}_{-0.5}$	$0.08^{+0.04}_{-0.01} {}^{+0.05}_{-0.04} \pm 0.01$
NR $_{1^{++}}(D^{*\mp}D^\pm)$	1^{++}	$17.8^{+1.9}_{-1.4} {}^{+3.6}_{-2.6}$	$16.1^{+1.7}_{-1.3} {}^{+3.3}_{-2.3}$	$1.21^{+0.13}_{-0.10} {}^{+0.24}_{-0.17} \pm 0.11$
NR $_{0^{++}}(D^{*\mp}D^\pm)$	0^{++}	$15.9^{+3.3}_{-1.2} {}^{+3.3}_{-3.3}$	$14.5^{+3.0}_{-1.1} {}^{+3.0}_{-3.0}$	$1.09^{+0.23}_{-0.08} {}^{+0.22}_{-0.23} \pm 0.09$

partial wave approach is also attempted, which results in a similar line shape but with large uncertainties due to the increased number of parameters. The shape based on the $\chi_{c1}(3872)$ tail is used in the baseline model. It should be stressed that this is considered as an effective model, rather than a description of genuine off-shell $\chi_{c1}(3872) \rightarrow D^{*\pm}D^\mp$ decays. A fit in which the mass and width parameters in Eq. (3) are free to vary fails due to very large interference with other 1^{++} states. Moreover, the measured $B^+ \rightarrow \text{EFF}_{1^{++}}K^+$, $\text{EFF}_{1^{++}} \rightarrow D^{*\pm}D^\mp$ branching fraction is determined to be $(1.48^{+0.41}_{-0.35}) \times 10^{-4}$, where all uncertainties are summed in quadrature. This value is larger than the measured branching fraction of $B^+ \rightarrow \chi_{c1}(3872)K^+$, $\chi_{c1}(3872) \rightarrow D^{*0}\bar{D}^0, \bar{D}^{*0}D^0$ [33], $(0.80 \pm 0.23) \times 10^{-4}$. Considering the smaller phase space available for $\chi_{c1}(3872) \rightarrow D^{*\pm}D^\mp$ decays, this indicates the contribution has a more complicated nature.

Four NR contributions are included to describe the $M(D^{*\pm}D^\mp)$ spectrum. The NR line shapes are $f_R(m) = 1$ except for NR $_{0^{++}}$, which is described by $f_R(m) = e^{(\alpha+\beta i)(m^2-m_0^2)}$ with $m_0 = 4.35$ GeV. The parameters α and β are determined from the fit to data to be 0.11 ± 0.03 GeV $^{-2}$ and -0.34 ± 0.05 GeV $^{-2}$, respectively, where the uncertainty is statistical only. For the NR $_{1^{++}}$ contribution, only the S -wave component is considered. The NR contributions amount to about 50% of the total fit fraction. Alternative models with fewer NR contributions, or NR amplitudes in the one or more of the $D^{(*)\pm}K^\pm$ systems,

are attempted but none provide agreement with the data comparable or better than that of the baseline model.

The two resonant contributions, $T_{\bar{c}\bar{s}0}^*(2870)^0$, and $T_{\bar{c}\bar{s}1}^*(2900)^0$, found in $B^+ \rightarrow D^+D^-K^+$ decays, are included in the $B^+ \rightarrow D^{*+}D^-K^+$ model to describe the enhancement seen in Fig. 1(e). The statistical significances of the $T_{\bar{c}\bar{s}0}^*(2870)^0$, and $T_{\bar{c}\bar{s}1}^*(2900)^0$ states are found to be 11σ and 9.2σ , respectively, thus confirming their existence in a new decay channel. If their parameters are left free in the fit, their values show some tension with the previous measurements, at the level of about 2σ when accounting for correlations, as seen in Table II. In addition, the ratio of the $T_{\bar{c}\bar{s}0}^*(2870)^0$, and $T_{\bar{c}\bar{s}1}^*(2900)^0$ branching fractions in this analysis is considerably larger than in the previous work. These tensions in the $T_{\bar{c}\bar{s}0,1}^*$ properties between $B^+ \rightarrow T_{\bar{c}\bar{s}0,1}^*D^+$ and $B^+ \rightarrow T_{\bar{c}\bar{s}0,1}^*D^{*+}$ decays may give further hints on the $T_{\bar{c}\bar{s}0,1}^*$ production mechanism.

The decay $T_{\bar{c}\bar{s}0}^*(2870)^0 \rightarrow D^{*-}K^+$ is forbidden by spin-parity conservation, while no clear contribution from $T_{\bar{c}\bar{s}1}^*(2900)^0$ is seen in Fig. 1(c). An upper limit on the fit fraction of $B^+ \rightarrow T_{\bar{c}\bar{s}1}^*(2900)^0D^+$, $T_{\bar{c}\bar{s}1}^*(2900)^0 \rightarrow D^{*-}K^+$ of 1.5% is set at 95% confidence level with statistical uncertainty only. This corresponds to an upper limit on $\mathcal{B}[T_{\bar{c}\bar{s}1}^*(2900)^0 \rightarrow D^{*-}K^+]/\mathcal{B}[T_{\bar{c}\bar{s}1}^*(2900)^0 \rightarrow D^-K^+]$ of 0.21 at 95% confidence level, using known values of the $B^+ \rightarrow D^+D^-K^+$ and $B^+ \rightarrow D^{*-}D^+K^+$ branching fractions [6,20]. Similarly, an upper limit on the fit fraction

TABLE II. Comparison of the $T_{\bar{c}s0,1}^{*0}$ properties obtained in this work to those found previously in $B^+ \rightarrow D^+ D^- K^+$ decays [2]. In the branching fractions determined in this work, the $T_{\bar{c}s0,1}^{*0}$ masses and widths are fixed to the previously measured values [2]. The branching fractions include the contributions of the $T_{\bar{c}s0,1}^{*0}$ decays.

Property	This work	Previous work
$T_{\bar{c}s0}^*(2870)^0$, mass [MeV]	$2914 \pm 11 \pm 15$	2866 ± 7
$T_{\bar{c}s0}^*(2870)^0$, width [MeV]	$128 \pm 22 \pm 23$	57 ± 13
$T_{\bar{c}s1}^*(2900)^0$ mass [MeV]	$2887 \pm 8 \pm 6$	2904 ± 5
$T_{\bar{c}s1}^*(2900)^0$ width [MeV]	$92 \pm 16 \pm 16$	110 ± 12
$\mathcal{B}[B^+ \rightarrow T_{\bar{c}s0}^*(2870)^0 D^{(*)+}]$	$(4.5_{-0.8}^{+0.6+0.9} \pm 0.4) \times 10^{-5}$	$(1.2 \pm 0.5) \times 10^{-5}$
$\mathcal{B}[B^+ \rightarrow T_{\bar{c}s1}^*(2900)^0 D^{(*)+}]$	$(3.8_{-1.0}^{+0.7+1.6} \pm 0.3) \times 10^{-5}$	$(6.7 \pm 2.3) \times 10^{-5}$
$\{\mathcal{B}[B^+ \rightarrow T_{\bar{c}s0}^*(2870)^0, D^{(*)+}]/\mathcal{B}[B^+ \rightarrow T_{\bar{c}s1}^*(2900)^0 D^{(*)+}]\}$	$1.17 \pm 0.31 \pm 0.48$	0.18 ± 0.05

of $B^+ \rightarrow T_{c\bar{s}0}^*(2900)^{++} D^{*-}$, $T_{c\bar{s}0}^*(2900)^{++} \rightarrow D^+ K^+$ of 3.3% is set at 95% confidence level.

In addition to the contributions discussed above, four extra charmonium(like) resonances are needed to describe the spectrum: $\eta_c(3945)$, $h_c(4000)$, $\chi_{c1}(4010)$, and $h_c(4300)$, with statistical significances found to be 10σ , 9.1σ , 16σ , and 6.4σ , respectively. When considering systematic uncertainties, the significance for the least significant, $h_c(4300)$, is 6.1σ . Their quantum numbers J^{PC} are determined to be 0^{-+} , 1^{+-} , 1^{++} , and 1^{+-} , respectively, with alternative J^{PC} values rejected with statistical significances of more than 5.7σ , while other measured properties are summarized in Table III. The assigned symbols are those for $I = 0$ states [3], as expected for charmonium resonances produced in $B^+ \rightarrow D^{*+} D^{\mp} K^+$ decays, but the isospin quantum number is not measured and exotic contributions are possible [35,36]. The mass and width of the $\eta_c(3945)$ resonance agree reasonably well with those of the previously reported $X(3940)$ state [9,10]. Given the measured quantum numbers, the state could be the $\eta_c(3S)$ state predicted in Ref. [34].

The fit results without the $h_c(4000)$, $\chi_{c1}(4010)$, and $h_c(4300)$ components are shown in Fig. 1 as green dashed

lines. The $h_c(4000)$ and $\chi_{c1}(4010)$ states are required to describe the discrepancy in $M(D^*D)$ around 4.0 GeV while the $h_c(4300)$ component is needed for the discrepancy around 4.3 GeV. The $h_c(4000)$ state has $C = -1$, which generates a distinctive interference pattern with the 1^{++} contributions, while the $\chi_{c1}(4010)$ component is required to describe the remaining discrepancy in this region (see Supplemental Material [39] for further details). The $h_c(4000)$ and $h_c(4300)$ resonances are potential candidates for the $h_c(2P)$ and $h_c(3P)$ states, respectively, and are the first reported candidates for these two charmonium states. The $h_c(4000)$ width is much larger than that of the charged $T_{c\bar{c}}(4020)^0$ state found by the BESIII Collaboration [37]. The $\chi_c(4274)$ state reported in Ref. [38], has mass and width close to those of the $h_c(4300)$ resonance but with different C parity. These are therefore likely to correspond to different charmonium states.

The $\chi_{c1}(4010)$ resonance has the expected J^{PC} quantum numbers of a χ_{c1} state. Its mass is, however, larger than those of the $\chi_{c1}(3872)$ and $\chi_{c2}(3930)$ states, and smaller than those of the $\chi_{c1}(4140)$ and $\chi_{c1}(4274)$ states. This may indicate that the $\chi_{c1}(4010)$ structure has exotic contributions [40–42].

TABLE III. Comparison of the charmonium(like) states found in this analysis with previously known states and the expected $c\bar{c}$ charmonium states with relevant J^{PC} quantum numbers as predicted in Ref. [34]. Units of MeV for masses and widths are implied.

This work		Known states [6]		$c\bar{c}$ prediction [34]	
$\eta_c(3945)$	$J^{PC} = 0^{-+}$	$X(3940)$ [9,10]	$J^{PC} = ?^{??}$	$\eta_c(3S)$	$J^{PC} = 0^{-+}$
$m_0 = 3945_{-17}^{+28+37}$	$\Gamma_0 = 130_{-49}^{+92+101}$	$m_0 = 3942 \pm 9$	$\Gamma_0 = 37_{-17}^{+27}$	$m_0 = 4064$	$\Gamma_0 = 80$
$h_c(4000)$	$J^{PC} = 1^{+-}$	$T_{c\bar{c}}(4020)^0$ [37]	$J^{PC} = ?^{?-}$	$h_c(2P)$	$J^{PC} = 1^{+-}$
$m_0 = 4000_{-14}^{+17+29}$	$\Gamma_0 = 184_{-45}^{+71+97}$	$m_0 = 4025.5_{-4.7}^{+2.0}$ ± 3.1	$\Gamma_0 = 23.0 \pm 6.0 \pm 1.0$	$m_0 = 3956$	$\Gamma_0 = 87$
$\chi_{c1}(4010)$	$J^{PC} = 1^{++}$			$\chi_{c1}(2P)$	$J^{PC} = 1^{++}$
$m_0 = 4012.5_{-3.9}^{+3.6+4.1}$	$\Gamma_0 = 62.7_{-6.4}^{+7.0+6.4}$			$m_0 = 3953$	$\Gamma_0 = 165$
$h_c(4300)$	$J^{PC} = 1^{+-}$			$h_c(3P)$	$J^{PC} = 1^{+-}$
$m_0 = 4307.3_{-6.6}^{+6.4+3.3}$	$\Gamma_0 = 58_{-16}^{+28+28}$			$m_0 = 4318$	$\Gamma_0 = 75$
		$\chi_c(4274)$ [38]	$J^{PC} = 1^{++}$	$\chi_{c1}(3P)$	$J^{PC} = 1^{++}$
		$m_0 = 4294 \pm 4_{-3}^{+6}$	$\Gamma_0 = 53 \pm 5 \pm 5$	$m_0 = 4317$	$\Gamma_0 = 39$

The agreement between the data and the baseline model is not perfect, with disagreements in two regions notable in Fig. 1. Firstly, an additional structure is seen around 4.4 GeV in the $M(D^*^-D^+)$ spectrum in Fig. 1(a), but not in the $M(D^{*+}D^-)$ distribution in Fig. 1(d). A new state is added to the model to test the significance of this structure. The best fit is obtained with mass 4462 ± 13 MeV, width 67 ± 18 MeV and $J^{PC} = 1^{++}$, where uncertainties are statistical only. The significance of this contribution is 3.7σ , and thus it is not included in the baseline model. The mass and width of this contribution are close to those of the $T_{c\bar{c}1}(4430)^0$ state; however, the charge and C parity are different. If the properties (except charge, C parity, and isospin) are fixed to those of the $T_{c\bar{c}1}(4430)^0$ state, the statistical significance of the component is 3.9σ , a higher significance compared to when those parameters are free in the fit since the look-elsewhere effect is not considered in this case.

Secondly, the baseline model exceeds the $M(D^{*-}K^+)$ data points in a broad range around 2.7 GeV in Fig. 1(c). If an additional $D^{*-}K^+$ resonance is added to the model to address this, the fit is unstable with the width taking very large values due to interference with the $NR_{0^+}(D^{*\mp}D^\pm)$ component. In a fit with the mass and width fixed to 2750 MeV and 100 MeV, respectively, the largest LL value improvement is around 30 units when the quantum numbers are $J^P = 1^+$. This indicates a deficiency with the baseline model, which is treated as a source of systematic uncertainty since it is not possible to establish whether it is due to an additional resonance or a mismodeling of one or more of the NR components.

Other previously observed states [43], including the $\psi(4160)$, $\chi_{c1}(4274)$, $\psi(4415)$, and $\psi(4660)$ resonances are also tested in the fit, but only improve the fit quality marginally and are therefore not included in the baseline fit model. Other possible contributions with free mass and width under different J^{PC} assumptions are also tested, and none of them improve the fit quality significantly.

The overall goodness of fit is quantified using binned χ^2 tests and the unbinned nearest neighbor method of Refs. [44,45]. These confirm the imperfect agreement between the data and the baseline model, with some metrics falling outside the 95% confidence level for the $B^+ \rightarrow D^{*-}D^+K^+$ mode. Acceptable goodness of fit, by these metrics, is obtained when the extra components mentioned above are included in the model. Since these potential extra components are treated as a source of systematic uncertainty, the quantitative impact of the discrepancies between data and the baseline fit model is considered to be accounted for in the results.

The main contributions in the $M(D^{*\pm}D^\mp)$ distribution are states with $J^P = 1^+$, which include one near-threshold contribution, three resonances, and one NR component in the baseline model. Constructive and destructive interference effects due to the different C parities of these

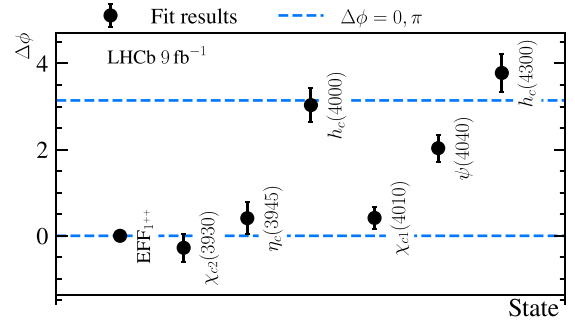


FIG. 2. Results of the C -parity determination, where $C_j = \pm 1$ is replaced by $\exp(i\Delta\phi_j)$. Uncertainties are statistical only.

contributions cause very different structures in Figs. 1(a) and 1(d). To validate the C -parity relationship, a further test is performed, which replaces the value of C parity in Eq. (2) with $\exp(i\Delta\phi)$, where $\Delta\phi$ is a free parameter for each resonance. In this test, the $EFF_{1^{++}}$ contribution is used as a reference to set the phase convention. Based on Eq. (2), the phase ϕ should be either $\Delta\phi = 0$ for $C = +$ or $\Delta\phi = \pi$ for $C = -$. The results are shown in Fig. 2. Clear separation between $C = +$ and $C = -$ states is found, with the fit results agreeing with the C parities assigned to the resonant contributions. The largest tension occurs for the $\psi(4040)$ state, which has phase 2.7σ away from the expected value of π when considering statistical uncertainty only. These results are robust against systematic variations, including the modeling of the $EFF_{1^{++}}$ line shape.

An alternative approach to describe the threshold enhancement is to replace the $EFF_{1^{++}}$ component with a $J^{PC} = 1^{++}$ contribution, modeled by the tail of $T_{c\bar{c}1}(3900)^0$ state. The two states lead to the same angular distributions, but their C parities are different. The C parities of other contributions, except $\chi_{c2}(3930)$ and $\psi(4040)$, are also changed. The alternative fit has an LL value that is worse than the baseline by 50 units, due to the unchanged C parities of the well-determined $\chi_{c2}(3930)$ and $\psi(4040)$ resonances [6]. It also results in very large NR contributions with exotic quantum numbers, which is considered unnatural. Thus, this hypothesis is rejected. Nonetheless, it is interesting to note that in this fit the new $h_c(4300)$ state from the baseline solution now has $J^{PC} = 1^{++}$, so that its parameters agree with those of the well-established $\chi_{c1}(4274)$ state. Additionally, the $\chi_{c1}(4010)$ properties become close to those of the previously observed $T_{c\bar{c}}(4020)^0$ state [37], with some tension on the width, while the $\eta_c(3945)$ state takes exotic quantum numbers $J^{PC} = 0^{-}$.

Systematic uncertainties due to limited precision on the background fraction, background modeling, efficiency map (including simulation sample size and uncertainties due to data-simulation corrections), and fixed parameters (i.e., resonance masses and widths) are estimated by generating pseudovalues (or distributions) according to

their uncertainties. The root mean squares of the fit results obtained with the newly generated settings are assigned as the related systematic uncertainties. Systematic uncertainties due to amplitude modeling are estimated by adding other known resonances and by adding an extra resonance with freely varying mass and width under different J^{PC} assumptions. The largest differences in fit results between all considered scenarios are assigned as the corresponding systematic uncertainties. The dominant systematic uncertainties on all measured quantities are those due to amplitude modeling.

In summary, a simultaneous amplitude analysis of $B^+ \rightarrow D^{*\pm} D^\mp K^+$ decays is performed for the first time. The analysis is based on a pp collision data sample collected by the LHCb experiment, corresponding to an integrated luminosity of 9 fb^{-1} , and exploits C -parity relations between contributions from charmonium(like) resonances in the two final states. The results provide new insights into charmonium(like) spectroscopy. Four charmonium(like) resonances, $\eta_c(3945)$, $h_c(4000)$, $\chi_{c1}(4010)$, and $h_c(4300)$, decaying into $D^{*\pm} D^\mp$, are observed, with J^{PC} values determined to be 0^{-+} , 1^{+-} , 1^{++} , and 1^{+-} , respectively. The $\eta_c(3945)$ resonance is found to be consistent with the previously observed $X(3940)$ state, while the other three are observed for the first time. In addition, the results confirm the existence of the $T_{\bar{c}\bar{s}0}^*(2870)^0$, and $T_{\bar{c}\bar{s}1}^*(2900)^0$ tetraquark states in new production channels, $B^+ \rightarrow D^{*+} T_{\bar{c}\bar{s}0,1}^*$. The ratio of branching fractions between $B^+ \rightarrow D^{*+} T_{\bar{c}\bar{s}0}^*(2870)^0$, and $B^+ \rightarrow D^{*+} T_{\bar{c}\bar{s}1}^*(2900)^0$ decays is larger than the corresponding value in $B^+ \rightarrow D^+ T_{\bar{c}\bar{s}0,1}^*$ decays, which may be of interest for understanding the nature of the $T_{\bar{c}\bar{s}0,1}^*$ states. Studies of additional $B \rightarrow D^{(*)} \bar{D}^{(*)} K$ processes and new theoretical investigations will be important to provide further insight into the structures observed in this analysis. This includes understanding the impacts of threshold effects and rescattering as well as determining the isospin of the different contributions [46].

Acknowledgments—We express our gratitude to our colleagues in the CERN accelerator departments for the excellent performance of the LHC. We thank the technical and administrative staff at the LHCb institutes. We acknowledge support from CERN and from the national agencies: CAPES, CNPq, FAPERJ, and FINEP (Brazil); MOST and NSFC (China); CNRS/IN2P3 (France); BMBF, DFG, and MPG (Germany); INFN (Italy); NWO (Netherlands); MNiSW and NCN (Poland); MCID/IFA (Romania); MICIU and AEI (Spain); SNSF and SER (Switzerland); NASU (Ukraine); STFC (United Kingdom); DOE NP and NSF (USA). We acknowledge the computing resources that are provided by CERN, IN2P3 (France), KIT and DESY (Germany), INFN (Italy), SURF (Netherlands), PIC (Spain), GridPP

(United Kingdom), CSCS (Switzerland), IFIN-HH (Romania), CBPF (Brazil), and Polish WLCG (Poland). We are indebted to the communities behind the multiple open-source software packages on which we depend. Individual groups or members have received support from ARC and ARDC (Australia); Key Research Program of Frontier Sciences of CAS, CAS PIFI, CAS CCEPP, Fundamental Research Funds for the Central Universities, and Sci. and Tech. Program of Guangzhou (China); Minciencias (Colombia); EPLANET, Marie Skłodowska-Curie Actions, ERC, and NextGenerationEU (European Union); A*MIDEX, ANR, IPhU, and Labex P2IO, and Région Auvergne-Rhône-Alpes (France); AvH Foundation (Germany); ICSC (Italy); Severo Ochoa and María de Maeztu Units of Excellence, GVA, XuntaGal, GENCAT, InTalent-Inditex and Prog. Atracción Talento CM (Spain); SRC (Sweden); the Leverhulme Trust, the Royal Society, and UKRI (United Kingdom).

-
- [1] R. Aaij *et al.* (LHCb Collaboration), Model-independent study of structure in $B^+ \rightarrow D^+ D^- K^+$ decays, *Phys. Rev. Lett.* **125**, 242001 (2020).
 - [2] R. Aaij *et al.* (LHCb Collaboration), Amplitude analysis of the $B^+ \rightarrow D^+ D^- K^+$ decay, *Phys. Rev. D* **102**, 112003 (2020).
 - [3] C. Amsler, E. Pianori, D. J. Robinson, and R. L. Workman, Naming scheme for hadrons, 2023. In Ref. [6], <https://pdg.lbl.gov/2023/reviews/rpp2023-rev-naming-scheme-hadrons.pdf>.
 - [4] R. Aaij *et al.* (LHCb Collaboration), First observation of a doubly charged tetraquark candidate and its neutral partner, *Phys. Rev. Lett.* **131**, 041902 (2023).
 - [5] R. Aaij *et al.* (LHCb Collaboration), Amplitude analysis of $B^0 \rightarrow \bar{D}^0 D_s^+ \pi^-$ and $B^+ \rightarrow D^- D_s^+ \pi^+$ decays, *Phys. Rev. D* **108**, 012017 (2023).
 - [6] R. L. Workman *et al.* (Particle Data Group), Review of particle physics, *Prog. Theor. Exp. Phys.* **2022**, 083C01 (2022), and 2023 update.
 - [7] N. Brambilla, S. Eidelman, C. Hanhart, A. Nefediev, C.-P. Shen, Christopher E. Thomas, A. Vairo, and C.-Z. Yuan, The XYZ states: Experimental and theoretical status and perspectives, *Phys. Rep.* **873**, 1 (2020).
 - [8] S. L. Olsen, T. Skwarnicki, and D. Zieminska, Nonstandard heavy mesons and baryons: Experimental evidence, *Rev. Mod. Phys.* **90**, 015003 (2018).
 - [9] K. Abe *et al.* (Belle Collaboration), Observation of a new charmonium state produced in association with a J/ψ in e^+e^- annihilation at $\sqrt{s} \approx 10.6 \text{ GeV}$, *Phys. Rev. Lett.* **98**, 082001 (2007).
 - [10] P. Pakhlov *et al.* (Belle Collaboration), Production of new charmoniumlike states in $e^+e^- \rightarrow J/\psi D^{(*)} \bar{D}^{(*)}$ at $\sqrt{s} \approx 10 \text{ GeV}$, *Phys. Rev. Lett.* **100**, 202001 (2008).
 - [11] M. Ablikim *et al.* (BESIII Collaboration), Observation of a neutral structure near the $D\bar{D}^*$ mass threshold in $e^+e^- \rightarrow (D\bar{D}^*)^0 \pi^0$ at $\sqrt{s} = 4.226$ and 4.257 GeV , *Phys. Rev. Lett.* **115**, 222002 (2015).

- [12] A. A. Alves Jr. *et al.* (LHCb Collaboration), The LHCb detector at the LHC, *J. Instrum.* **3**, S08005 (2008).
- [13] R. Aaij *et al.* (LHCb Collaboration), LHCb detector performance, *Int. J. Mod. Phys. A* **30**, 1530022 (2015).
- [14] T. Sjöstrand, S. Mrenna, and P. Skands, A brief introduction to PYTHIA8.1, *Comput. Phys. Commun.* **178**, 852 (2008); T. Sjöstrand, S. Mrenna, and P. Skands, PYTHIA6.4 physics and manual, *J. High Energy Phys.* **05** (2006) 026.
- [15] I. Belyaev *et al.*, Handling of the generation of primary events in Gauss, the LHCb simulation framework, *J. Phys. Conf. Ser.* **331**, 032047 (2011).
- [16] D. J. Lange, The EvtGen particle decay simulation package, *Nucl. Instrum. Methods Phys. Res., Sect. A* **462**, 152 (2001).
- [17] N. Davidson, T. Przedzinski, and Z. Was, PHOTOS interface in C++: Technical and physics documentation, *Comput. Phys. Commun.* **199**, 86 (2016).
- [18] J. Allison *et al.* (Geant4 Collaboration), GEANT4 developments and applications, *IEEE Trans. Nucl. Sci.* **53**, 270 (2006); S. Agostinelli *et al.* (Geant4 Collaboration), GEANT4: A simulation toolkit, *Nucl. Instrum. Methods Phys. Res., Sect. A* **506**, 250 (2003).
- [19] M. Clemencic, G. Corti, S. Easo, C. R. Jones, S. Miglioranza, M. Pappagallo, and P. Robbe, The LHCb simulation application, Gauss: Design, evolution and experience, *J. Phys. Conf. Ser.* **331**, 032023 (2011).
- [20] R. Aaij *et al.* (LHCb Collaboration), Measurement of branching fraction ratios for $B^+ \rightarrow D^{*+}D^-K^+$, $B^+ \rightarrow D^{*-}D^+K^+$, and $B^0 \rightarrow D^{*-}D^0K^+$ decays, *J. High Energy Phys.* **12** (2020) 139.
- [21] L. Breiman, J. H. Friedman, R. A. Olshen, and C. J. Stone, *Classification and Regression Trees* (Wadsworth International Group, Belmont, California, USA, 1984).
- [22] Y. Freund and R. E. Schapire, A decision-theoretic generalization of on-line learning and an application to boosting, *J. Comput. Syst. Sci.* **55**, 119 (1997).
- [23] H. Voss, A. Hoecker, J. Stelzer, and F. Tegenfeldt, TMVA—Toolkit for multivariate data analysis with ROOT, *Proc. Sci., ACAT2007* (2007) 040; A. Hoecker *et al.*, TMVA4—toolkit for multivariate data analysis with ROOT. Users guide, [arXiv: physics/0703039](https://arxiv.org/abs/physics/0703039).
- [24] A. Garmash *et al.* (Belle Collaboration), Dalitz analysis of the three-body charmless decays $B^+ \rightarrow K^+\pi^+\pi^-$ and $B^+ \rightarrow K^+K^+K^-$, *Phys. Rev. D* **71**, 092003 (2005).
- [25] L. Anderlini *et al.*, The PIDCalib package, Report No. LHCb-PUB-2016-021, 2016.
- [26] LHCb Collaboration, LHCb tracker upgrade technical design report, Report No. CERN-LHCC-2014-001, 2014.
- [27] S. Tolk, J. Albrecht, F. Dettori, and A. Pellegrino, Data driven trigger efficiency determination at LHCb, Report No. LHCb-PUB-2014-039, 2014.
- [28] J. M. Blatt and V. F. Weisskopf, *Theoretical Nuclear Physics* (Springer, New York, 1952).
- [29] J. Back *et al.*, LAURA⁺⁺: A Dalitz plot fitter, *Comput. Phys. Commun.* **231**, 198 (2018).
- [30] E. Gross and O. Vitells, Trial factors for the look elsewhere effect in high energy physics, *Eur. Phys. J. C* **70**, 525 (2010).
- [31] S. Algeri, J. Conrad, D. A. van Dyk, and B. Anderson, On methods for correcting for the look-elsewhere effect in searches for new physics, *J. Instrum.* **11**, P12010 (2016).
- [32] B. Efron, Bootstrap methods: Another look at the jackknife, *Ann. Stat.* **7** (1979) 1.
- [33] T. Aushev *et al.* (Belle Collaboration), Study of the $B \rightarrow X(3872)(\rightarrow D^{*0}\bar{D}^0)K$ decay, *Phys. Rev. D* **81**, 031103 (2010).
- [34] T. Barnes, S. Godfrey, and E. S. Swanson, Higher charmonia, *Phys. Rev. D* **72**, 054026 (2005).
- [35] X.-K. Dong, F.-K. Guo, and B.-S. Zou, A survey of heavy-antiheavy hadronic molecules, *Prog. Phys.* **41**, 65 (2021).
- [36] J. F. Giron, R. F. Lebed, and S. R. Martinez, Spectrum of hidden-charm, open-strange exotics in the dynamical diquark model, *Phys. Rev. D* **104**, 054001 (2021).
- [37] M. Ablikim *et al.* (BESIII Collaboration), Observation of a neutral charmoniumlike state $Z_c(4025)^0$ in $e^+e^- \rightarrow (D^*\bar{D}^*)^0\pi^0$, *Phys. Rev. Lett.* **115**, 182002 (2015).
- [38] R. Aaij *et al.* (LHCb Collaboration), Observation of new resonances decaying to $J/\psi K^+$ and $J/\psi\phi$, *Phys. Rev. Lett.* **127**, 082001 (2021).
- [39] See Supplemental Material at <http://link.aps.org/supplemental/10.1103/PhysRevLett.133.131902> for the difference between the $M(D^*D)$ distributions of the $B^+ \rightarrow D^{*+}D^-K^+$ and $B^+ \rightarrow D^{*-}D^+K^+$ decays with fit results superimposed and the results of fits with and without the $h_c(4000)$, $\chi_{c1}(4010)$ and $h_c(4300)$ contributions.
- [40] G.-J. Wang *et al.*, New insight into the exotic states strongly coupled with the $D\bar{D}^*$ from the T_{cc}^+ , [arXiv:2306.12406](https://arxiv.org/abs/2306.12406).
- [41] Q. Deng, R.-H. Ni, Q. Li, and X.-H. Zhong, Charmonia in an unquenched quark model, [arXiv:2312.10296](https://arxiv.org/abs/2312.10296).
- [42] H. Li *et al.*, $X(3872)$ relevant $D\bar{D}^*$ scattering in $N_f = 2$ lattice QCD, [arXiv:2402.14541](https://arxiv.org/abs/2402.14541).
- [43] V. Zhukova *et al.* (Belle Collaboration), Angular analysis of the $e^+e^- \rightarrow D^{(*)\pm}D^{*\mp}$ process near the open charm threshold using initial-state radiation, *Phys. Rev. D* **97**, 012002 (2018).
- [44] M. Williams, How good are your fits? Unbinned multivariate goodness-of-fit tests in high energy physics, *J. Instrum.* **5**, P09004 (2010).
- [45] P. J. Bickel and L. Breiman, Sums of functions of nearest neighbor distances, moment bounds, limit theorems and a goodness of fit test, *Ann. Probab.* **11**, 185 (1983).
- [46] A. E. Bondar and A. I. Milstein, Charge asymmetry in decays $B \rightarrow D\bar{D}K$, *J. High Energy Phys.* **12** (2020) 015.

R. Aaij³⁶, A. S. W. Abdelmotteleb⁵⁵, C. Abellan Beteta⁴⁹, F. Abudinén⁵⁵, T. Ackernley⁵⁹, A. A. Adefisoye⁶⁷, B. Adeva⁴⁵, M. Adinolfi⁵³, P. Adlarson⁷⁹, C. Agapopoulou⁴⁷, C. A. Aidala⁸⁰, Z. Ajaltouni¹¹, S. Akar⁶⁴, K. Akiba³⁶, P. Albicocco²⁶, J. Albrecht¹⁸, F. Alessio⁴⁷, M. Alexander⁵⁸, Z. Aliouche⁶¹, P. Alvarez Cartelle⁵⁴, R. Amalric¹⁵, S. Amato³, J. L. Amey⁵³, Y. Amhis^{13,47}, L. An⁶, L. Anderlini²⁵, M. Andersson⁴⁹

A. Andreianov⁴², P. Andreola⁴⁹, M. Andreotti²⁴, D. Andreou⁶⁷, A. Anelli^{29,b}, D. Ao⁷, F. Archilli^{35,c},
 M. Argenton²⁴, S. Arguedas Cuendis⁹, A. Artamonov⁴², M. Artuso⁶⁷, E. Aslanides¹², M. Atzeni⁶³,
 B. Audurier¹⁴, D. Bacher⁶², I. Bachiller Perea¹⁰, S. Bachmann²⁰, M. Bachmayer⁴⁸, J. J. Back⁵⁵,
 P. Baladron Rodriguez⁴⁵, V. Balagura¹⁴, W. Baldini²⁴, J. Baptista de Souza Leite⁵⁹, M. Barbetti^{25,d},
 I. R. Barbosa⁶⁸, R. J. Barlow⁶¹, S. Barsuk¹³, W. Barter⁵⁷, M. Bartolini⁵⁴, J. Bartz⁶⁷, F. Baryshnikov⁴²,
 J. M. Basels¹⁶, G. Bassi^{33,s}, B. Batsukh⁵, A. Battig¹⁸, A. Bay⁴⁸, A. Beck⁵⁵, M. Becker¹⁸, F. Bedeschi³³,
 I. B. Bediaga², A. Beiter⁶⁷, S. Belin⁴⁵, V. Bellee⁴⁹, K. Belous⁴², I. Belov²⁷, I. Belyaev³⁴, G. Benane¹²,
 G. Bencivenni²⁶, E. Ben-Haim¹⁵, A. Berezhnoy⁴², R. Bernet⁴⁹, S. Bernet Andres⁴³, C. Bertella⁶¹, A. Bertolin³¹,
 C. Betancourt⁴⁹, F. Betti⁵⁷, J. Bex⁵⁴, Ia. Bezshyiko⁴⁹, J. Bhom³⁹, M. S. Bieker¹⁸, N. V. Biesuz²⁴, P. Billoir¹⁵,
 A. Biolchini³⁶, M. Birch⁶⁰, F. C. R. Bishop¹⁰, A. Bitadze⁶¹, A. Bizzeti²⁰, T. Blake⁵⁵, F. Blanc⁴⁸, J. E. Blank¹⁸,
 S. Blusk⁶⁷, V. Bocharnikov⁴², J. A. Boelhauve¹⁸, O. Boente Garcia¹⁴, T. Boettcher⁶⁴, A. Bohare⁵⁷,
 A. Boldyrev⁴², C. S. Bolognani⁷⁶, R. Bolzonella^{24,e}, N. Bondar⁴², F. Borgato^{31,47,f}, S. Borghi⁶¹, M. Borsato^{29,b},
 J. T. Borsuk³⁹, S. A. Bouchiba⁴⁸, T. J. V. Bowcock⁵⁹, A. Boyer⁴⁷, C. Bozzi²⁴, M. J. Bradley⁶⁰,
 A. Brea Rodriguez⁴⁵, N. Breer¹⁸, J. Brodzicka³⁹, A. Brossa Gonzalo⁴⁵, J. Brown⁵⁹, D. Brundu³⁰, E. Buchanan⁵⁷,
 A. Buonaura⁴⁹, L. Buonincontri^{31,f}, A. T. Burke⁶¹, C. Burr⁴⁷, A. Bursche⁷⁰, A. Butkevich⁴², J. S. Butter⁵⁴,
 J. Buytaert⁴⁷, W. Byczynski⁴⁷, S. Cadeddu³⁰, H. Cai⁷², R. Calabrese^{24,e}, L. Calefice⁴⁴, S. Cali²⁶, M. Calvi^{29,b},
 M. Calvo Gomez⁴³, J. I. Cambon Bouzas⁴⁵, P. Campana²⁶, D. H. Campora Perez⁷⁶, A. F. Campoverde Quezada⁷,
 S. Capelli²⁹, L. Capriotti²⁴, R. Caravaca-Mora⁹, A. Carbone^{23,g}, L. Carcedo Salgado⁴⁵, R. Cardinale^{27,h},
 A. Cardini³⁰, P. Carniti^{29,b}, L. Carus²⁰, A. Casais Vidal⁶³, R. Caspary²⁰, G. Casse⁵⁹, J. Castro Godinez⁹,
 M. Cattaneo⁴⁷, G. Cavallero^{24,47}, V. Cavallini^{24,e}, S. Celani²⁰, J. Cerasoli¹², D. Cervenkov⁶², S. Cesare^{28,i},
 A. J. Chadwick⁵⁹, I. Chahrour⁸⁰, M. Charles¹⁵, Ph. Charpentier⁴⁷, C. A. Chavez Barajas⁵⁹, M. Chefdeville¹⁰,
 C. Chen¹², S. Chen⁵, Z. Chen⁷, A. Chernov³⁹, S. Chernyshenko⁵¹, V. Chobanova⁷⁸, S. Cholak⁴⁸,
 M. Chrzaszcz³⁹, A. Chubykin⁴², V. Chulikov⁴², P. Ciambone²⁶, X. Cid Vidal⁴⁵, G. Ciezarek⁴⁷, P. Cifra⁴⁷,
 P. E. L. Clarke⁵⁷, M. Clemencic⁴⁷, H. V. Cliff⁵⁴, J. Closier⁴⁷, C. Cocha Toapaxi²⁰, V. Coco⁴⁷, J. Cogan¹²,
 E. Cogneras¹¹, L. Cojocariu⁴¹, P. Collins⁴⁷, T. Colombo⁴⁷, A. Comerma-Montells⁴⁴, L. Congedo²², A. Contu³⁰,
 N. Cooke⁵⁸, I. Corredoira⁴⁵, A. Correia¹⁵, G. Corti⁴⁷, J. J. Cottee Meldrum⁵³, B. Couturier⁴⁷, D. C. Craik⁴⁹,
 M. Cruz Torres^{2,j}, E. Curras Rivera⁴⁸, R. Currie⁵⁷, C. L. Da Silva⁶⁶, S. Dadabaev⁴², L. Dai⁶⁹, X. Dai⁶,
 E. Dall'Occo¹⁸, J. Dalseno⁴⁵, C. D'Ambrosio⁴⁷, J. Daniel¹¹, A. Danilina⁴², P. d'Argent²², A. Davidson⁵⁵,
 J. E. Davies⁶¹, A. Davis⁶¹, O. De Aguiar Francisco⁶¹, C. De Angelis^{30,k}, F. De Benedetti⁴⁷, J. de Boer³⁶,
 K. De Bruyn⁷⁵, S. De Capua⁶¹, M. De Cian^{20,47}, U. De Freitas Carneiro Da Graca^{2,l}, E. De Lucia²⁶,
 J. M. De Miranda², L. De Paula³, M. De Serio^{22,m}, P. De Simone²⁶, F. De Vellis¹⁸, J. A. de Vries⁷⁶,
 F. Debernardis²², D. Decamp¹⁰, V. Dedu¹², L. Del Buono¹⁵, B. Delaney⁶³, H.-P. Dembinski¹⁸, J. Deng⁸,
 V. Denysenko⁴⁹, O. Deschamps¹¹, F. Dettori^{30,k}, B. Dey⁷⁴, P. Di Nezza²⁶, I. Diachkov⁴², S. Didenko⁴²,
 S. Ding⁶⁷, L. Dittmann²⁰, V. Dobishuk⁵¹, A. D. Docheva⁵⁸, A. Dolmatov⁴², C. Dong⁴, A. M. Donohoe²¹,
 F. Dordei³⁰, A. C. dos Reis², A. D. Dowling⁶⁷, A. G. Downes¹⁰, W. Duan⁷⁰, P. Duda⁷⁷, M. W. Dudek³⁹,
 L. Dufour⁴⁷, V. Duk³², P. Durante⁴⁷, M. M. Duras⁷⁷, J. M. Durham⁶⁶, O. D. Durmus⁷⁴, A. Dziurda³⁹,
 A. Dzyuba⁴², S. Easo⁵⁶, E. Eckstein¹⁷, U. Egede¹, A. Egorychev⁴², V. Egorychev⁴², S. Eisenhardt⁵⁷, E. Ejopu⁶¹,
 S. Ek-In⁴⁸, L. Eklund⁷⁹, M. Elashri⁶⁴, J. Ellbracht¹⁸, S. Ely⁶⁰, A. Ene⁴¹, E. Eppe⁶⁴, S. Escher¹⁶, J. Eschle⁶⁷,
 S. Esen²⁰, T. Evans⁶¹, F. Fabiano^{30,47,k}, L. N. Falcao², Y. Fan⁷, B. Fang^{72,13}, L. Fantini^{32,n}, M. Faria⁴⁸,
 K. Farmer⁵⁷, D. Fazzini^{29,b}, L. Felkowski⁷⁷, M. Feng^{5,7}, M. Feo^{18,47}, M. Fernandez Gomez⁴⁵, A. D. Fernandez⁶⁵,
 F. Ferrari²³, F. Ferreira Rodrigues³, S. Ferreres Sole³⁶, M. Ferrillo⁴⁹, M. Ferro-Luzzi⁴⁷, S. Filippov⁴²,
 R. A. Fini²², M. Fiorini^{24,e}, K. M. Fischer⁶², D. S. Fitzgerald⁸⁰, C. Fitzpatrick⁶¹, F. Fleuret¹⁴, M. Fontana²³,
 L. F. Foreman⁶¹, R. Forty⁴⁷, D. Foulds-Holt⁵⁴, M. Franco Sevilla⁶⁵, M. Frank⁴⁷, E. Franzoso^{24,e}, G. Frau²⁰,
 C. Frei⁴⁷, D. A. Friday⁶¹, J. Fu⁷, Q. Fuehring¹⁸, Y. Fujii¹, T. Fulghesu¹⁵, E. Gabriel³⁶, G. Galati^{22,m},
 M. D. Galati³⁶, A. Gallas Torreira⁴⁵, D. Galli^{23,g}, S. Gambetta⁵⁷, M. Gandelman³, P. Gandini²⁸, H. Gao⁷,
 R. Gao⁶², Y. Gao⁸, Y. Gao⁶, Y. Gao⁸, M. Garau^{30,k}, L. M. Garcia Martin⁴⁸, P. Garcia Moreno⁴⁴,
 J. García Pardiñas⁴⁷, K. G. Garg⁸, L. Garrido⁴⁴, C. Gaspar⁴⁷, R. E. Geertsema³⁶, L. L. Gerken¹⁸, E. Gersabeck⁶¹,
 M. Gersabeck⁶¹, T. Gershon⁵⁵, Z. Ghorbanimoghaddam⁵³, L. Giambastiani^{31,f}, F. I. Giasemis^{15,o}, V. Gibson⁵⁴,
 H. K. Giemza⁴⁰, A. L. Gilman⁶², M. Giovannetti²⁶, A. Gioventù⁴⁴, P. Gironella Gironell⁴⁴, C. Giugliano^{24,e}

M. A. Giza³⁹, E. L. Gkougkousis⁶⁰, F. C. Glaser^{13,20}, V. V. Gligorov¹⁵, C. Göbel⁶⁸, E. Golobardes⁴³,
 D. Golubkov⁴², A. Golutvin^{60,42,47}, A. Gomes^{2,a,p}, S. Gomez Fernandez⁴⁴, F. Goncalves Abrantes⁶²,
 M. Goncerz³⁹, G. Gong⁴, J. A. Gooding¹⁸, I. V. Gorelov⁴², C. Gotti²⁹, J. P. Grabowski¹⁷,
 L. A. Granado Cardoso⁴⁷, E. Graugés⁴⁴, E. Graverini^{48,q}, L. Grazette⁵⁵, G. Graziani⁴, A. T. Grecu⁴¹,
 L. M. Greeven³⁶, N. A. Grieser⁶⁴, L. Grillo⁵⁸, S. Gromov⁴², C. Gu¹⁴, M. Guarise²⁴, M. Guittiere¹³,
 V. Guliaeva⁴², P. A. Günther²⁰, A.-K. Guseinov⁴⁸, E. Gushchin⁴², Y. Guz^{6,42,47}, T. Gys⁴⁷, K. Habermann¹⁷,
 T. Hadavizadeh¹, C. Hadjivasiliou⁶⁵, G. Haefeli⁴⁸, C. Haen⁴⁷, J. Haimberger⁴⁷, M. Hajheidari⁴⁷,
 M. M. Halvorsen⁴⁷, P. M. Hamilton⁶⁵, J. Hammerich⁵⁹, Q. Han⁸, X. Han²⁰, S. Hansmann-Menzemer²⁰, L. Hao⁷,
 N. Harnew⁶², T. Harrison⁵⁹, M. Hartmann¹³, J. He^{7,r}, F. Hemmer⁴⁷, C. Henderson⁶⁴, R. D. L. Henderson^{1,55},
 A. M. Hennequin⁴⁷, K. Hennessy⁵⁹, L. Henry⁴⁸, J. Herd⁶⁰, P. Herrero Gascon²⁰, J. Heuel¹⁶, A. Hicheur³,
 G. Hijano Mendizabal⁴⁹, D. Hill⁴⁸, S. E. Hollitt¹⁸, J. Horswill⁶¹, R. Hou⁸, Y. Hou¹¹, N. Howarth⁵⁹, J. Hu²⁰,
 J. Hu⁷⁰, W. Hu⁶, X. Hu⁴, W. Huang⁷, W. Hulsbergen³⁶, R. J. Hunter⁵⁵, M. Hushchyn⁴², D. Hutchcroft⁵⁹,
 D. Ilin⁴², P. Ilten⁶⁴, A. Inglessi⁴², A. Iniukhin⁴², A. Ishteev⁴², K. Ivshin⁴², R. Jacobsson⁴⁷, H. Jage¹⁶,
 S. J. Jaimes Elles^{46,73}, S. Jakobsen⁴⁷, E. Jans³⁶, B. K. Jashal⁴⁶, A. Jawahery^{65,47}, V. Jevtic¹⁸, E. Jiang⁶⁵,
 X. Jiang^{5,7}, Y. Jiang⁷, Y. J. Jiang⁶, M. John⁶², D. Johnson⁵², C. R. Jones⁵⁴, T. P. Jones⁵⁵, S. Joshi⁴⁰, B. Jost⁴⁷,
 N. Jurik⁴⁷, I. Juszczak³⁹, D. Kaminaris⁴⁸, S. Kandybei⁵⁰, Y. Kang⁴, M. Karacson⁴⁷, D. Karpenkov⁴²,
 A. Kauniskangas⁴⁸, J. W. Kautz⁶⁴, F. Keizer⁴⁷, M. Kenzie⁵⁴, T. Ketel³⁶, B. Khanji⁶⁷, A. Kharisova⁴²,
 S. Kholodenko^{33,47}, G. Khreich¹³, T. Kirn¹⁶, V. S. Kirsebom^{29,b}, O. Kitouni⁶³, S. Klaver³⁷, N. Kleijne^{33,s},
 K. Klimaszewski⁴⁰, M. R. Kmiec⁴⁰, S. Koliiev⁵¹, L. Kolk¹⁸, A. Konoplyannikov⁴², P. Kopciwicz^{38,47},
 P. Koppenburg³⁶, M. Korolev⁴², I. Kostiuk³⁶, O. Kot⁵¹, S. Kotriakhova⁴², A. Kozachuk⁴², P. Kravchenko⁴²,
 L. Kravchuk⁴², M. Kreps⁵⁵, S. Kretschmar¹⁶, P. Krovovny⁴², W. Krupa⁶⁷, W. Krzemien⁴⁰, J. Kubat²⁰,
 S. Kubis⁷⁷, W. Kucewicz³⁹, M. Kucharczyk³⁹, V. Kudryavtsev⁴², E. Kulikova⁴², A. Kupsc⁷⁹, B. K. Kutsenko¹²,
 D. Lacarrere⁴⁷, A. Lai³⁰, A. Lampis³⁰, D. Lancierini⁵⁴, C. Landesa Gomez⁴⁵, J. J. Lane¹, R. Lane⁵³,
 C. Langenbruch²⁰, J. Langer¹⁸, O. Lantwin⁴², T. Latham⁵⁵, F. Lazzari^{33,q}, C. Lazzeroni⁵², R. Le Gac¹²,
 R. Lefèvre¹¹, A. Leflat⁴², S. Legotin⁴², M. Lehuraux⁵⁵, E. Lemos Cid⁴⁷, O. Leroy¹², T. Lesiak³⁹,
 B. Leverington²⁰, A. Li⁴, H. Li⁷⁰, K. Li⁸, L. Li⁶¹, P. Li⁴⁷, P.-R. Li⁷¹, S. Li⁸, T. Li^{5,1}, T. Li⁷⁰, Y. Li⁸, Y. Li⁵,
 Z. Li⁶⁷, Z. Lian⁴, X. Liang⁶⁷, S. Libralon⁴⁶, C. Lin⁷, T. Lin⁵⁶, R. Lindner⁴⁷, V. Lisovskyi⁴⁸, R. Litvinov³⁰,
 F. L. Liu¹, G. Liu⁷⁰, K. Liu⁷¹, Q. Liu⁷, S. Liu^{5,7}, Y. Liu⁵⁷, Y. Liu⁷¹, Y. L. Liu⁶⁰, A. Lobo Salvia⁴⁴, A. Loi³⁰,
 J. Lomba Castro⁴⁵, T. Long⁵⁴, J. H. Lopes³, A. Lopez Huertas⁴⁴, S. López Soliño⁴⁵, C. Lucarelli^{25,d},
 D. Lucchesi^{31,f}, M. Lucio Martinez⁷⁶, V. Lukashenko^{36,51}, Y. Luo⁶, A. Lupato³¹, E. Luppi^{24,e}, K. Lynch²¹,
 X.-R. Lyu⁷, G. M. Ma⁴, R. Ma⁷, S. Maccolini¹⁸, F. Machefert¹³, F. Maciuc⁴¹, B. Mack⁶⁷, I. Mackay⁶²,
 L. M. Mackey⁶⁷, L. R. Madhan Mohan⁵⁴, M. J. Madurai⁵², A. Maevskiy⁴², D. Magdalinski³⁶, D. Maisuzenko⁴²,
 M. W. Majewski³⁸, J. J. Malczewski³⁹, S. Malde⁶², B. Malecki³⁹, L. Malentacca⁴⁷, A. Malinin⁴², T. Maltsev⁴²,
 G. Manca^{30,k}, G. Mancinelli¹², C. Mancuso^{28,13,i}, R. Manera Escalero⁴⁴, D. Manuzzi²³, D. Marangotto^{28,i},
 J. F. Marchand¹⁰, R. Marchevski⁴⁸, U. Marconi²³, S. Mariani⁴⁷, C. Marin Benito⁴⁴, J. Marks²⁰,
 A. M. Marshall⁵³, P. J. Marshall⁵⁹, G. Martelli^{32,n}, G. Martellotti³⁴, L. Martinazzoli⁴⁷, M. Martinelli^{29,b},
 D. Martinez Santos⁴⁵, F. Martinez Vidal⁴⁶, A. Massafferri², M. Materok¹⁶, R. Matev⁴⁷, A. Mathad⁴⁷,
 V. Matiunin⁴², C. Matteuzzi⁶⁷, K. R. Mattioli¹⁴, A. Mauri⁶⁰, E. Maurice¹⁴, J. Mauricio⁴⁴, P. Mayencourt⁴⁸,
 M. Mazurek⁴⁰, M. McCann⁶⁰, L. Mcconnell²¹, T. H. McGrath⁶¹, N. T. McHugh⁵⁸, A. McNab⁶¹, R. McNulty²¹,
 B. Meadows⁶⁴, G. Meier¹⁸, D. Melnychuk⁴⁰, M. Merk^{36,76}, A. Merli^{28,i}, L. Meyer Garcia³, D. Miao^{5,7},
 H. Miao⁷, M. Mikhasenko^{17,u}, D. A. Milanes⁷³, A. Minotti^{29,b}, E. Minucci⁶⁷, T. Miralles¹¹, B. Mitreska¹⁸,
 D. S. Mitzel¹⁸, A. Modak⁵⁶, A. Mödden¹⁸, R. A. Mohammed⁶², R. D. Moise¹⁶, S. Mokhnenko⁴², T. Mombächer⁴⁷,
 M. Monk^{55,1}, S. Monteil¹¹, A. Morcillo Gomez⁴⁵, G. Morello²⁶, M. J. Morello^{33,s}, M. P. Morgenthaler²⁰,
 A. B. Morris⁴⁷, A. G. Morris¹², R. Mountain⁶⁷, H. Mu⁴, Z. M. Mu⁶, E. Muhammad⁵⁵, F. Muheim⁵⁷,
 M. Mulder⁷⁵, K. Müller⁴⁹, F. Muñoz-Rojas⁹, R. Murta⁶⁰, P. Naik⁵⁹, T. Nakada⁴⁸, R. Nandakumar⁵⁶, T. Nanut⁴⁷,
 I. Nasteva³, M. Needham⁵⁷, N. Neri^{28,i}, S. Neubert¹⁷, N. Neufeld⁴⁷, P. Neustroev⁴², J. Nicolini^{18,13}, D. Nicotra⁷⁶,
 E. M. Niel⁴⁸, N. Nikitin⁴², P. Nogga¹⁷, N. S. Nolte⁶³, C. Normand⁵³, J. Novoa Fernandez⁴⁵, G. Nowak⁶⁴,
 C. Nunez⁸⁰, H. N. Nur⁵⁸, A. Oblakowska-Mucha³⁸, V. Obraztsov⁴², T. Oeser¹⁶, S. Okamura^{24,47,e},
 A. Okhotnikov⁴², R. Oldeman^{30,k}, F. Oliva⁵⁷, M. Olocco¹⁸, C. J. G. Onderwater⁷⁶, R. H. O'Neil⁵⁷

J. M. Otalora Goicochea³ P. Owen⁴⁹ A. Oyanguren⁴⁶ O. Ozcelik⁵⁷ K. O. Padeken¹⁷ B. Pagare⁵⁵ P. R. Pais²⁰
T. Pajero⁶² A. Palano²² M. Palutan²⁶ G. Panshin⁴² L. Paolucci⁵⁵ A. Papanestis⁵⁶ M. Pappagallo^{22,m}
L. L. Pappalardo^{24,e} C. Pappenheimer⁶⁴ C. Parkes⁶¹ B. Passalacqua²⁴ G. Passaleva²⁵ D. Passaro^{33,s}
A. Pastore²² M. Patel⁶⁰ J. Patoc⁶² C. Patrignani^{23,g} C. J. Pawley⁷⁶ A. Pellegrino³⁶ M. Pepe Altarelli²⁶
S. Perazzini²³ D. Pereima⁴² A. Pereiro Castro⁴⁵ P. Perret¹¹ A. Perro⁴⁷ K. Petridis⁵³ A. Petrolini^{27,h}
S. Petrucci⁵⁷ J. P. Pfaller⁶⁴ H. Pham⁶⁷ L. Pica^{33,s} M. Piccini³² B. Pietrzyk¹⁰ G. Pietrzyk¹³ D. Pinci³⁴
F. Pisani⁴⁷ M. Pizzichemi^{29,b} V. Placinta⁴¹ M. Plo Casasus⁴⁵ F. Polci^{15,47} M. Poli Lener²⁶ A. Poluektov¹²
N. Polukhina⁴² E. Polycarpo³ S. Ponce⁴⁷ D. Popov⁷ S. Poslavskii⁴² K. Prasanth³⁹ C. Prouve⁴⁵
V. Pugatch⁵¹ G. Punzi^{33,q} W. Qian⁷ N. Qin⁴ S. Qu⁴ R. Quagliani⁴⁸ R. I. Rabadan Trejo⁵⁵
J. H. Rademacker⁵³ M. Rama³³ M. Ramírez García⁸⁰ M. Ramos Pernas⁵⁵ M. S. Rangel³ F. Ratnikov⁴²
G. Raven³⁷ M. Rebollo De Miguel⁴⁶ F. Redi^{28,v} J. Reich⁵³ F. Reiss⁶¹ Z. Ren⁷ P. K. Resmi⁶² R. Ribatti^{33,s}
G. R. Ricart^{14,81} D. Riccardi^{33,s} S. Ricciardi⁵⁶ K. Richardson⁶³ M. Richardson-Slipper⁵⁷ K. Rinnert⁵⁹
P. Robbe¹³ G. Robertson⁵⁸ E. Rodrigues⁵⁹ E. Rodriguez Fernandez⁴⁵ J. A. Rodriguez Lopez⁷³
E. Rodriguez Rodriguez⁴⁵ A. Rogovskiy⁵⁶ D. L. Rolf⁴⁷ P. Roloff⁴⁷ V. Romanovskiy⁴² M. Romero Lamas⁴⁵
A. Romero Vidal⁴⁵ G. Romolini²⁴ F. Ronchetti⁴⁸ M. Rotondo²⁶ S. R. Roy²⁰ M. S. Rudolph⁶⁷ T. Ruf⁴⁷
M. Ruiz Diaz²⁰ R. A. Ruiz Fernandez⁴⁵ J. Ruiz Vidal^{79,w} A. Ryzhikov⁴² J. Ryzka³⁸ J. J. Saavedra-Arias⁹
J. J. Saborido Silva⁴⁵ R. Sadek¹⁴ N. Sagidova⁴² D. Sahoo⁷⁴ N. Sahoo⁵² B. Saitta^{30,k} M. Salomoni^{29,47,b}
C. Sanchez Gras³⁶ I. Sanderswood⁴⁶ R. Santacesaria³⁴ C. Santamarina Rios⁴⁵ M. Santimaria²⁶ L. Santoro²
E. Santovetti³⁵ A. Saputi^{24,47} D. Saranin⁴² G. Sarpis⁵⁷ M. Sarpis¹⁷ A. Sarti³⁴ C. Satriano^{34,x} A. Satta³⁵
M. Saur⁶ D. Savrina⁴² H. Sazak¹⁶ L. G. Scantlebury Smead⁶² A. Scarabotto¹⁸ S. Schael¹⁶ S. Scherl⁵⁹
M. Schiller⁵⁸ H. Schindler⁴⁷ M. Schmelling¹⁹ B. Schmidt⁴⁷ S. Schmitt¹⁶ H. Schmitz¹⁷ O. Schneider⁴⁸
A. Schopper⁴⁷ N. Schulte¹⁸ S. Schulte⁴⁸ M. H. Schune¹³ R. Schwemmer⁴⁷ G. Schwering¹⁶ B. Sciascia²⁶
A. Sciuccati⁴⁷ S. Sellam⁴⁵ A. Semennikov⁴² T. Senger⁴⁹ M. Senghi Soares³⁷ A. Sergi²⁷ N. Serra⁴⁹
L. Sestini³¹ A. Seuthe¹⁸ Y. Shang⁶ D. M. Shangase⁸⁰ M. Shapkin⁴² R. S. Sharma⁶⁷ I. Shchemerov⁴²
L. Shchutska⁴⁸ T. Shears⁵⁹ L. Shekhtman⁴² Z. Shen⁶ S. Sheng^{5,7} V. Shevchenko⁴² B. Shi⁷ Q. Shi⁷
E. B. Shields^{29,b} Y. Shimizu¹³ E. Shmanin⁴² R. Shorkin⁴² J. D. Shupperd⁶⁷ R. Silva Coutinho⁶⁷ G. Simi^{31,f}
S. Simone^{22,m} N. Skidmore⁵⁵ T. Skwarnicki⁶⁷ M. W. Slater⁵² J. C. Smallwood⁶² E. Smith⁶³ K. Smith⁶⁶
M. Smith⁶⁰ A. Snoch³⁶ L. Soares Lavra⁵⁷ M. D. Sokoloff⁶⁴ F. J. P. Soler⁵⁸ A. Solomin^{42,53} A. Solovov⁴²
I. Solovyev⁴² R. Song¹ Y. Song⁴⁸ Y. Song⁴ Y. S. Song⁶ F. L. Souza De Almeida⁶⁷ B. Souza De Paula³
E. Spadaro Norella^{28,i} E. Spedicato²³ J. G. Speer¹⁸ E. Spiridenkov⁴² P. Spradlin⁵⁸ V. Sriskaran⁴⁷ F. Stagni⁴⁷
M. Stahl⁴⁷ S. Stahl⁴⁷ S. Stanislaus⁶² E. N. Stein⁴⁷ O. Steinkamp⁴⁹ O. Stenyakin⁴² H. Stevens¹⁸
D. Strelakina⁴² Y. Su⁷ F. Suljik⁶² J. Sun³⁰ L. Sun⁷² Y. Sun⁶⁵ W. Sutcliffe⁴⁹ P. N. Swallow⁵² F. Swystun⁵⁴
A. Szabelski⁴⁰ T. Szumlak³⁸ Y. Tan⁴ M. D. Tat⁶² A. Terentev⁴⁹ F. Terzuoli^{33,y} F. Teubert⁴⁷ E. Thomas⁴⁷
D. J. D. Thompson⁵² H. Tilquin⁶⁰ V. Tisserand¹¹ S. T'Jampens¹⁰ M. Tobin⁵ L. Tomassetti^{24,e}
G. Tonani^{28,47,i} X. Tong⁶ D. Torres Machado² L. Toscano¹⁸ D. Y. Tou⁴ C. Tripll⁴³ G. Tuci²⁰ N. Tuning³⁶
L. H. Uecker²⁰ A. Ukleja³⁸ D. J. Unverzagt²⁰ E. Ursov⁴² A. Usachov³⁷ A. Ustyuzhanin⁴² U. Uwer²⁰
V. Vagnoni²³ A. Valassi⁴⁷ G. Valenti²³ N. Valls Canudas⁴⁷ H. Van Hecke⁶⁶ E. van Herwijnen⁶⁰
C. B. Van Hulse^{45,z} R. Van Laak⁴⁸ M. van Veghel³⁶ G. Vasquez⁴⁹ R. Vazquez Gomez⁴⁴ P. Vazquez Regueiro⁴⁵
C. Vázquez Sierra⁴⁵ S. Vecchi²⁴ J. J. Velthuis⁵³ M. Veltri^{25,aa} A. Venkateswaran⁴⁸ M. Vesterinen⁵⁵
M. Vieites Diaz⁴⁷ X. Vilasis-Cardona⁴³ E. Vilella Figueras⁵⁹ A. Villa²³ P. Vincent¹⁵ F. C. Volle⁵²
D. vom Bruch¹² V. Vorobyev⁴² N. Voropaev⁴² K. Vos⁷⁶ G. Vouters¹⁰ C. Vrahas⁵⁷ J. Wagner¹⁸ J. Walsh³³
E. J. Walton^{1,55} G. Wan⁶ C. Wang²⁰ G. Wang⁸ J. Wang⁶ J. Wang⁵ J. Wang⁴ J. Wang⁷² M. Wang²⁸
N. W. Wang⁷ R. Wang⁵³ X. Wang⁷⁰ X. W. Wang⁶⁰ Y. Wang⁸ Z. Wang¹³ Z. Wang⁴ Z. Wang²⁸
J. A. Ward^{55,1} M. Waterlaat⁴⁷ N. K. Watson⁵² D. Websdale⁶⁰ Y. Wei⁶ B. D. C. Westhenry⁵³ D. J. White⁶¹
M. Whitehead⁵⁸ A. R. Wiederhold⁵⁵ D. Wiedner¹⁸ G. Wilkinson⁶² M. K. Wilkinson⁶⁴ M. Williams⁶³
M. R. J. Williams⁵⁷ R. Williams⁵⁴ F. F. Wilson⁵⁶ W. Wislicki⁴⁰ M. Witek³⁹ L. Witola²⁰ C. P. Wong⁶⁶
G. Wormser¹³ S. A. Wotton⁵⁴ H. Wu⁶⁷ J. Wu⁸ Y. Wu⁶ K. Wyllie⁴⁷ S. Xian⁷⁰ Z. Xiang⁵ Y. Xie⁸ A. Xu³³
J. Xu⁷ L. Xu⁴ L. Xu⁴ M. Xu⁵⁵ Z. Xu¹¹ Z. Xu⁷ Z. Xu⁵ D. Yang⁴ S. Yang⁷ X. Yang⁶ Y. Yang^{27,h}
Z. Yang⁶ Z. Yang⁶⁵ V. Yeroshenko¹³ H. Yeung⁶¹ H. Yin⁸ C. Y. Yu⁶ J. Yu⁶⁹ X. Yuan⁵ E. Zaffaroni⁴⁸

M. Zavertyaev¹⁹, M. Zdybal³⁹, M. Zeng⁴, C. Zhang⁶, D. Zhang⁸, J. Zhang⁷, L. Zhang⁴, S. Zhang⁶⁹,
 S. Zhang⁶, Y. Zhang⁶, Y. Z. Zhang⁴, Y. Zhao²⁰, A. Zharkova⁴², A. Zhelezov²⁰, X. Z. Zheng⁴, Y. Zheng⁷,
 T. Zhou⁶, X. Zhou⁸, Y. Zhou⁷, V. Zhovkovska⁵⁵, L. Z. Zhu⁷, X. Zhu⁴, X. Zhu⁸, V. Zhukov¹⁶, J. Zhuo⁴⁶,
 Q. Zou^{5,7}, D. Zuliani^{31,f} and G. Zunica⁴⁸

(LHCb Collaboration)

¹*School of Physics and Astronomy, Monash University, Melbourne, Australia*

²*Centro Brasileiro de Pesquisas Físicas (CBPF), Rio de Janeiro, Brazil*

³*Universidade Federal do Rio de Janeiro (UFRJ), Rio de Janeiro, Brazil*

⁴*Center for High Energy Physics, Tsinghua University, Beijing, China*

⁵*Institute Of High Energy Physics (IHEP), Beijing, China*

⁶*School of Physics State Key Laboratory of Nuclear Physics and Technology, Peking University, Beijing, China*

⁷*University of Chinese Academy of Sciences, Beijing, China*

⁸*Institute of Particle Physics, Central China Normal University, Wuhan, Hubei, China*

⁹*Consejo Nacional de Rectores (CONARE), San Jose, Costa Rica*

¹⁰*Université Savoie Mont Blanc, CNRS, IN2P3-LAPP, Annecy, France*

¹¹*Université Clermont Auvergne, CNRS/IN2P3, LPC, Clermont-Ferrand, France*

¹²*Aix Marseille Univ, CNRS/IN2P3, CPPM, Marseille, France*

¹³*Université Paris-Saclay, CNRS/IN2P3, IJCLab, Orsay, France*

¹⁴*Laboratoire Leprince-Ringuet, CNRS/IN2P3, Ecole Polytechnique, Institut Polytechnique de Paris, Palaiseau, France*

¹⁵*LPNHE, Sorbonne Université, Paris Diderot Sorbonne Paris Cité, CNRS/IN2P3, Paris, France*

¹⁶*I. Physikalisches Institut, RWTH Aachen University, Aachen, Germany*

¹⁷*Universität Bonn - Helmholtz-Institut für Strahlen und Kernphysik, Bonn, Germany*

¹⁸*Fakultät Physik, Technische Universität Dortmund, Dortmund, Germany*

¹⁹*Max-Planck-Institut für Kernphysik (MPIK), Heidelberg, Germany*

²⁰*Physikalisches Institut, Ruprecht-Karls-Universität Heidelberg, Heidelberg, Germany*

²¹*School of Physics, University College Dublin, Dublin, Ireland*

²²*INFN Sezione di Bari, Bari, Italy*

²³*INFN Sezione di Bologna, Bologna, Italy*

²⁴*INFN Sezione di Ferrara, Ferrara, Italy*

²⁵*INFN Sezione di Firenze, Firenze, Italy*

²⁶*INFN Laboratori Nazionali di Frascati, Frascati, Italy*

²⁷*INFN Sezione di Genova, Genova, Italy*

²⁸*INFN Sezione di Milano, Milano, Italy*

²⁹*INFN Sezione di Milano-Bicocca, Milano, Italy*

³⁰*INFN Sezione di Cagliari, Monserrato, Italy*

³¹*INFN Sezione di Padova, Padova, Italy*

³²*INFN Sezione di Perugia, Perugia, Italy*

³³*INFN Sezione di Pisa, Pisa, Italy*

³⁴*INFN Sezione di Roma La Sapienza, Roma, Italy*

³⁵*INFN Sezione di Roma Tor Vergata, Roma, Italy*

³⁶*Nikhef National Institute for Subatomic Physics, Amsterdam, Netherlands*

³⁷*Nikhef National Institute for Subatomic Physics and VU University Amsterdam, Amsterdam, Netherlands*

³⁸*AGH - University of Krakow, Faculty of Physics and Applied Computer Science, Kraków, Poland*

³⁹*Henryk Niewodniczanski Institute of Nuclear Physics Polish Academy of Sciences, Kraków, Poland*

⁴⁰*National Center for Nuclear Research (NCBJ), Warsaw, Poland*

⁴¹*Horia Hulubei National Institute of Physics and Nuclear Engineering, Bucharest-Magurele, Romania*

⁴²*Affiliated with an institute covered by a cooperation agreement with CERN*

⁴³*DS4DS, La Salle, Universitat Ramon Llull, Barcelona, Spain*

⁴⁴*ICCUB, Universitat de Barcelona, Barcelona, Spain*

⁴⁵*Instituto Galego de Física de Altas Enerxías (IGFAE), Universidade de Santiago de Compostela, Santiago de Compostela, Spain*

⁴⁶*Instituto de Fisica Corpuscular, Centro Mixto Universidad de Valencia - CSIC, Valencia, Spain*

⁴⁷*European Organization for Nuclear Research (CERN), Geneva, Switzerland*

⁴⁸*Institute of Physics, Ecole Polytechnique Fédérale de Lausanne (EPFL), Lausanne, Switzerland*

⁴⁹*Physik-Institut, Universität Zürich, Zürich, Switzerland*

⁵⁰*NSC Kharkiv Institute of Physics and Technology (NSC KIPT), Kharkiv, Ukraine*

⁵¹*Institute for Nuclear Research of the National Academy of Sciences (KINR), Kyiv, Ukraine*

- ⁵²*University of Birmingham, Birmingham, United Kingdom*
- ⁵³*H.H. Wills Physics Laboratory, University of Bristol, Bristol, United Kingdom*
- ⁵⁴*Cavendish Laboratory, University of Cambridge, Cambridge, United Kingdom*
- ⁵⁵*Department of Physics, University of Warwick, Coventry, United Kingdom*
- ⁵⁶*STFC Rutherford Appleton Laboratory, Didcot, United Kingdom*
- ⁵⁷*School of Physics and Astronomy, University of Edinburgh, Edinburgh, United Kingdom*
- ⁵⁸*School of Physics and Astronomy, University of Glasgow, Glasgow, United Kingdom*
- ⁵⁹*Oliver Lodge Laboratory, University of Liverpool, Liverpool, United Kingdom*
- ⁶⁰*Imperial College London, London, United Kingdom*
- ⁶¹*Department of Physics and Astronomy, University of Manchester, Manchester, United Kingdom*
- ⁶²*Department of Physics, University of Oxford, Oxford, United Kingdom*
- ⁶³*Massachusetts Institute of Technology, Cambridge, MA, United States*
- ⁶⁴*University of Cincinnati, Cincinnati, OH, United States*
- ⁶⁵*University of Maryland, College Park, MD, United States*
- ⁶⁶*Los Alamos National Laboratory (LANL), Los Alamos, NM, United States*
- ⁶⁷*Syracuse University, Syracuse, NY, United States*
- ⁶⁸*Pontifícia Universidade Católica do Rio de Janeiro (PUC-Rio), Rio de Janeiro, Brazil
(associated with Universidade Federal do Rio de Janeiro (UFRJ), Rio de Janeiro, Brazil)*
- ⁶⁹*School of Physics and Electronics, Hunan University, Changsha City, China
(associated with Institute of Particle Physics, Central China Normal University, Wuhan, Hubei, China)*
- ⁷⁰*Guangdong Provincial Key Laboratory of Nuclear Science, Guangdong-Hong Kong Joint Laboratory of Quantum Matter,
Institute of Quantum Matter, South China Normal University, Guangzhou, China
(associated with Center for High Energy Physics, Tsinghua University, Beijing, China)*
- ⁷¹*Lanzhou University, Lanzhou, China
(associated with Institute Of High Energy Physics (IHEP), Beijing, China)*
- ⁷²*School of Physics and Technology, Wuhan University, Wuhan, China
(associated with Center for High Energy Physics, Tsinghua University, Beijing, China)*
- ⁷³*Departamento de Física, Universidad Nacional de Colombia, Bogota, Colombia
(associated with LPNHE, Sorbonne Université, Paris Diderot Sorbonne Paris Cité, CNRS/IN2P3, Paris, France)*
- ⁷⁴*Eotvos Lorand University, Budapest, Hungary
(associated with European Organization for Nuclear Research (CERN), Geneva, Switzerland)*
- ⁷⁵*Van Swinderen Institute, University of Groningen, Groningen, Netherlands
(associated with Nikhef National Institute for Subatomic Physics, Amsterdam, Netherlands)*
- ⁷⁶*Universiteit Maastricht, Maastricht, Netherlands
(associated with Nikhef National Institute for Subatomic Physics, Amsterdam, Netherlands)*
- ⁷⁷*Tadeusz Kosciuszko Cracow University of Technology, Cracow, Poland
(associated with Henryk Niewodniczanski Institute of Nuclear Physics Polish Academy of Sciences, Kraków, Poland)*
- ⁷⁸*Universidad da Coruña, A Coruna, Spain
(associated with DS4DS, La Salle, Universitat Ramon Llull, Barcelona, Spain)*
- ⁷⁹*Department of Physics and Astronomy, Uppsala University, Uppsala, Sweden
(associated with School of Physics and Astronomy, University of Glasgow, Glasgow, United Kingdom)*
- ⁸⁰*University of Michigan, Ann Arbor, MI, United States
(associated with Syracuse University, Syracuse, NY, United States)*
- ⁸¹*Departement de Physique Nucleaire (SPhN), Gif-Sur-Yvette, France*

^aDeceased.

^bAlso at Università degli Studi di Milano-Bicocca, Milano, Italy.

^cAlso at Università di Roma Tor Vergata, Roma, Italy.

^dAlso at Università di Firenze, Firenze, Italy.

^eAlso at Università di Ferrara, Ferrara, Italy.

^fAlso at Università di Padova, Padova, Italy.

^gAlso at Università di Bologna, Bologna, Italy.

^hAlso at Università di Genova, Genova, Italy.

ⁱAlso at Università degli Studi di Milano, Milano, Italy.

^jAlso at Universidad Nacional Autónoma de Honduras, Tegucigalpa, Honduras.

^kAlso at Università di Cagliari, Cagliari, Italy.

^lAlso at Centro Federal de Educação Tecnológica Celso Suckow da Fonseca, Rio De Janeiro, Brazil.

^mAlso at Università di Bari, Bari, Italy.

ⁿAlso at Università di Perugia, Perugia, Italy.

^oAlso at LIP6, Sorbonne Université, Paris, France.

^pAlso at Universidade de Brasília, Brasília, Brazil.

^qAlso at Università di Pisa, Pisa, Italy.

^rAlso at Hangzhou Institute for Advanced Study, UCAS, Hangzhou, China.

^sAlso at Scuola Normale Superiore, Pisa, Italy.

^tAlso at School of Physics and Electronics, Henan University, Kaifeng, China.

^uAlso at Excellence Cluster ORIGINS, Munich, Germany.

^vAlso at Università degli studi di Bergamo, Bergamo, Italy.

^wAlso at Department of Physics/Division of Particle Physics, Lund, Sweden.

^xAlso at Università della Basilicata, Potenza, Italy.

^yAlso at Università di Siena, Siena, Italy.

^zAlso at Universidad de Alcalá, Alcalá de Henares, Spain.

^{aa}Also at Università di Urbino, Urbino, Italy.